Orbital polarization in manganese oxides

Ryo Maezono, Sumio Ishihara,* and Naoto Nagaosa
Department of Applied Physics, University of Tokyo, Bunkyo-ku, Tokyo 113, Japan
(Received 17 February 1998)

We study the role of orbital degrees of freedom in perovskite manganites, which are well known as colossal-magnetoresistance (CMR) compounds. The double degeneracy of the e_g orbitals is treated with isospin. Orbital polarization is essential to explain the variety of phases in these compounds and their physical properties. Especially important is the fact that the orbital is aligned as $d_{x^2-y^2}$ in the metallic layered antiferromagnetic state, which explains the experimentally observed quasi-two-dimensional transport and absence of spin canting. A large orbital fluctuation in the ferromagnetic state is also predicted. [S0163-1829(98)52122-4]

The discovery of colossal magnetoresistance (CMR) in manganese oxides $R_{1-x}A_x\mathrm{MnO}_3$ (R: rare-earth metal ion, A: divalent metal ion) has revived the interest in these materials.[1] In these compounds the most important interaction is the double exchange interaction, which gives a close interplay between the spin and charge dymanics.[2–5] However, the other degrees of freedom, i.e., the orbital, play important roles, which we address in this paper. In the conventional models of these materials,[2–5] the twofold degeneracy of the e_g orbitals has been often neglected assuming that the basic physics remain unchanged from the single orbital case. However, due to recent intensive studies, several important features have been revealed which cannot be understood in terms of these simplified models. Especially the phase diagrams are rich including various antiferromagnetic structures in addition to the ferromagnetic one as shown in Fig. 1. In $\mathrm{Nd}_{1-x}\mathrm{Sr}_x\mathrm{MnO}_3$ the metallic spin: A state [layered antiferromagnetic (AF)] is found in the region $0.5<x<0.6$.[7,6] There is no spin canting observed in the neutron experiments, which is in disagreement with de Gennes's theory.[4] For $x>0.6$ the C-type (rod-type AF) magnetic structure appears.[6] We found that this rich phase diagram and some physical properties can be understood only when the orbital polarization is taken into account.

Because the Coulomb interaction is the strongest interaction and also the Jahn-Teller (JT) distortion disappears for $x>0.15$,[8] we first study the model with only electron-electron interactions:

$$H=\sum_{\langle ij\rangle,\sigma,\gamma,\gamma'}(t_{ij}^{\gamma\gamma'}d_{i\gamma\sigma}^{\dagger}d_{j\gamma'\sigma}+\mathrm{H.c.})+U\sum_{i\gamma}n_{i\gamma\uparrow}n_{i\gamma\downarrow}+U'\sum_{i}n_{ia}n_{ib}+I\sum_{i,\sigma,\sigma'}d_{ia\sigma}^{\dagger}d_{ib\sigma'}^{\dagger}d_{ia\sigma'}d_{ib\sigma}+J_H\sum_{i}\vec{S}_i\cdot\vec{S}_i^{t_{2g}}+J_s\sum_{\langle ij\rangle}\vec{S}_i^{t_{2g}}\cdot\vec{S}_j^{t_{2g}}. \quad (1)$$

$d_{i\gamma\sigma}^{\dagger}$ is the operator which creates an electron with spin $\sigma(=\uparrow,\downarrow)$ in orbital $\gamma(=a,b)$ at site i, and $\vec{S}_i$ is the spin operator for the e_g electron defined by $\vec{S}_i=\frac{1}{2}\Sigma_{\sigma\sigma'\gamma}d_{i\sigma\gamma}^{\dagger}\vec{\sigma}_{\sigma\sigma'}d_{i\sigma'\gamma}$. $\vec{S}_i^{t_{2g}}$ is the spin operator for t_{2g} spin with $S=3/2$. The electron transfer integral $t_{ij}^{\gamma\gamma'}$ is estimated by considering the oxygen $2p$ orbitals between the nearest Mn-Mn pair. It is represented as $c_{ij}^{\gamma\gamma'}t_0$, where $c_{ij}^{\gamma\gamma'}$ is the numerical factor depending on the orbitals and t_0 is estimated to be 0.72 eV which we choose as the unit of energy below ($t_0=1$).[9] The second line is the electron-electron interactions, where U, U', and I are the intraorbital, interorbital Coulomb interactions, and interorbital exchange interaction, respectively. These interactions can be rewritten as $-\alpha\Sigma_i(\vec{S}_i+(J_H/2\alpha)\vec{S}_i^{t_{2g}})^2-\beta\Sigma_i\vec{T}_i^2$.[10] Here the spin operator $\vec{S}_i$ and the isospin operator $\vec{T}_i=\frac{1}{2}\Sigma_{\gamma\gamma'\sigma}d_{i\sigma\gamma}^{\dagger}\vec{\sigma}_{\gamma\gamma'}d_{i\sigma\gamma'}$ for the orbital degrees of freedom are introduced, and the two positive coefficients α and β, which are defined by $\alpha=2U/3+U'/3-I/6$ and $\beta=U'-I/2$, represent the interaction to induce the spin and isospin moments, respectively. The last line in Eq. (1) is the sum of the Hund coupling (J_H) and the antiferromagnetic (AF) interaction (J_s) between the nearest-neighboring t_{2g} spins.

We adopt the mean-field approximation with the order parameters $\langle\vec{S}_i\rangle$, $\langle\vec{S}_i^{t_{2g}}\rangle$, and $\langle\vec{T}_i\rangle$. These order parameters are determined to optimize the mean-field energy at zero temperature. Here it is noted that both the super exchange and the double exchange interactions are taken into account in a unified fashion in this mean-field theory. The energy

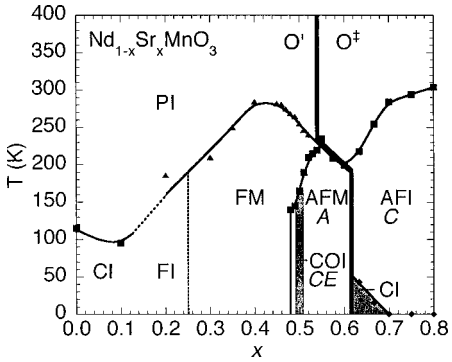

FIG. 1. The experimental phase diagram for $\mathrm{Nd}_{1-x}\mathrm{Sr}_x\mathrm{MnO}_3$. (Ref. 6) CI is the insulator with canted spin structure. It is basically A-type for $0.0<x<0.1$ while it is C-type in the small region for $0.6<x<0.7$. PI (FI) is the paramagnetic (ferromagnetic) insulator, and FM is the ferromagnetic metal. COI is the charge ordered insulator with CE-type AF order.

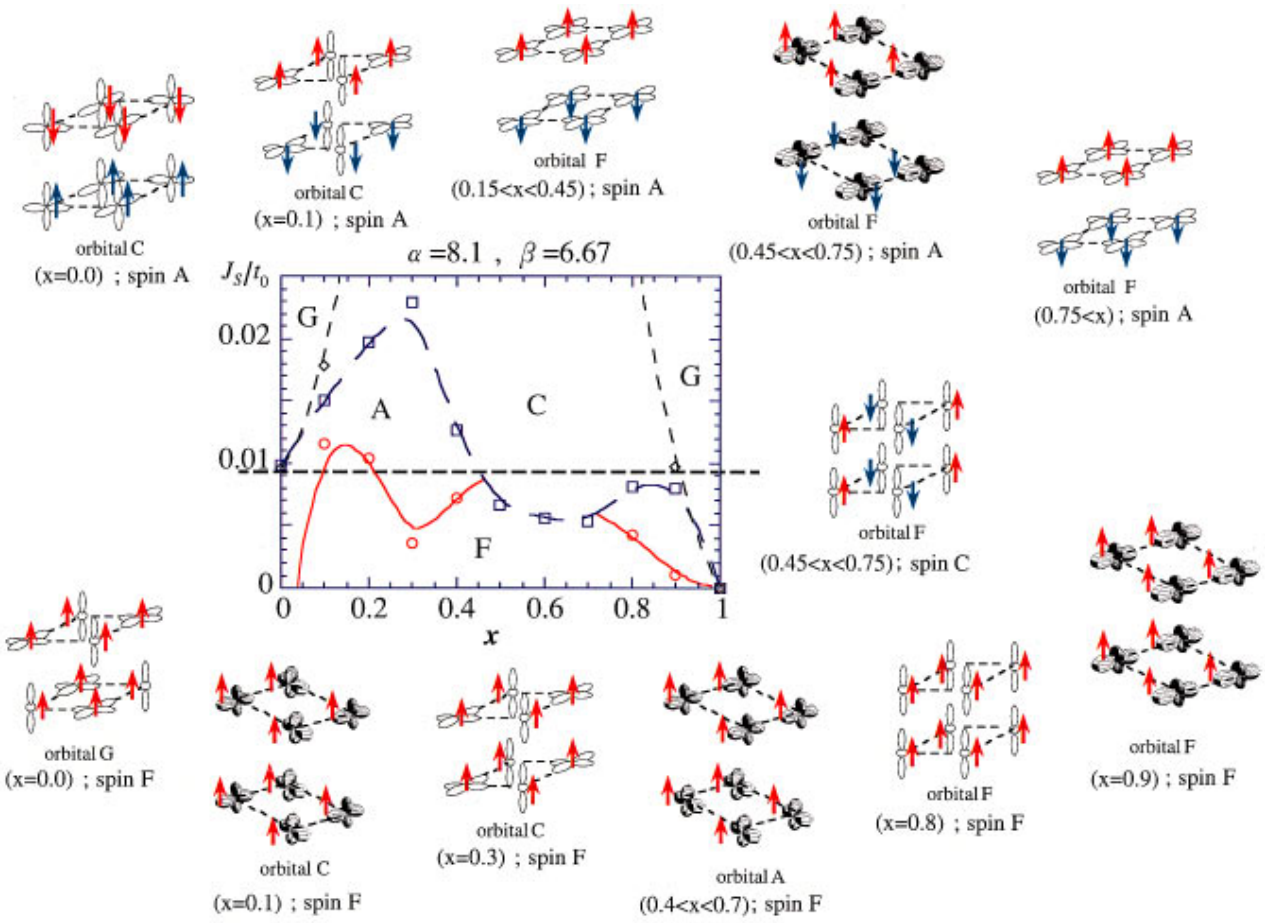

FIG. 2. (Color) The calculated phase diagram in the plane of the carrier concentration (x) and the antiferromagnetic interaction J_s between the t_{2g} spins. The strength of the interactions are set as $\alpha=8.1t_0$ and $\beta=6.67t_0$. With these parameters both the spin and orbital moments are almost fully polarized. The schematic orbital structure in each phase is also shown.

gain due to the former interaction corresponds to change in the center of mass for the occupied states due to the hybridization with the unoccupied states, while the latter to the energy of the doped hole at the top of the occupied states. As x increases the relative importance of these two interactions is changed gradually, i.e., the double exchange interaction becomes more important. For both spin and orbital, the four types of the ordering are considered, that is, the ferromagnetic (F-type) ordering, where the order parameters are uniform, and the three AF orderings, i.e., the layer-type (A-type), the rod-type (C-type), and the NaCl-type (G-type) AF orderings. Hereafter, types of the orderings are termed as, for example, spin:C, and so on.

In Fig. 2, the calculated phase diagram is shown in the plane of x (the concentration of the holes) and J_s (the super exchange interaction between the t_{2g} spins) for the set of parameters $\alpha=8.1t_0$, $\beta=6.67t_0$. This corresponds to the realistic values of $U=8.75t_0$, $U'=7.35t_0$, and $I=1.4t_0$. With these values of interactions both the spin and orbital moments are fully polarized. The orbital structure is shown in each region of the phase diagram. The phase boundary J_s(FA) between the A and F spin structures is nonmonotonic. Although the value of J_s cannot be estimated accurately at the moment, there are two rough estimates. One is from the Néel transition temperature T_N for $CaMnO_3$ ($x=1.0$), which suggests $J_s=T_N/7.5\cong 0.8$ meV$\cong 0.001t_0$ in the mean-field approximation.[11] The fluctuations will lower T_N, and hence increase the estimate for J_s. Another estimate is obtained from the numerical calculations for $LaMnO_3$ ($x=0.0$), which suggests $J_s\cong 8$ meV$\cong 0.011t_0$.[9] From these we estimate J_s roughly of the order of $\sim 0.01J_s$. Although J_s might depend on x in real materials, we tentatively fix J_s to be $0.009t_0$ represented by the broken line in Fig. 2. Then the

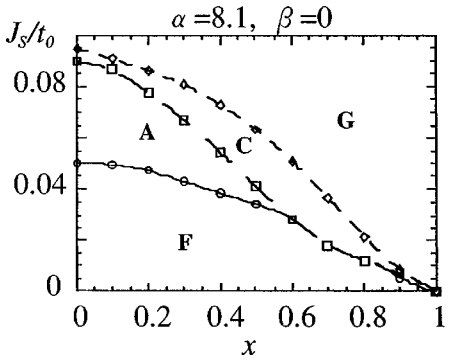

FIG. 3. The calculated mean-field phase diagram with $\alpha=8.1t_0$ and $\beta=0.0$. The orbital moment is not polarized in this case.

spin structure is changed as A→F→A→C→G, as x increases, which is in good agreement with the experiments shown in Fig. 1. This seems more remarkable when we compare it with the phase diagram with $\beta=0$, i.e., in the case of no orbital polarization, in Fig. 3. In this case the ferromagnetic state is dominating for the reasonable value of J_s and nonmonotonic behavior does not appear. Then we conclude that the the orbital polarization due to the large interorbital Coulomb interaction is essential to reproduce the observed phase diagram.

Now let us discuss the phase diagram in Fig. 2 in more detail. The spin:A phase for $x=0$ is stabilized by the super exchange interaction. The most stable orbital structure there is orbital:G $(y^2-z^2)/(z^2-x^2)$ as shown in Fig. 2. The experimentally supposed orbital:G $(3x^2-r^2)/(3y^2-r^2)$ is higher in energy due to the following reason. There are three possibilities for the intermediate states of the super exchange process, i.e., occupancy of two e_g orbitals (a) with the parallel spins (the energy $U'-I$), or (b) antiparallel spins $(U'+I)$, and (c) the double occupancies of the same orbital (U).[9,12] Let us compare the energy gains due to the super exchange processes in orbital:G $(y^2-z^2)/(z^2-x^2)$ and orbital:G $(3x^2-r^2)/(3y^2-r^2)$. For the processes using states (a) and (b), magnitudes of the transfer integrals and hence the energy gain are the same, while for the process using (c), the energy gain is always larger for $(y^2-z^2)/(z^2-x^2)$ compared with $(3x^2-r^2)/(3y^2-r^2)$ because of the anisotropic transfer integrals along the c axis. Hence the JT coupling is important in addition to the electron-electron interactions at $x=0$. We then introduce the JT distortion observed experimentally and its coupling to the e_g electrons. The energy splitting g between two e_g orbitals is introduced as a parameter. It is shown that the wave functions become almost $(3x^2-r^2)/(3y^2-r^2)$ when g is about half of the transfer energy t_0. This value is much smaller than what is expected in the absence of the electron-electron interactions. This is because the orbital moment $|\vec{T}_i|$ is already fully induced by the electron-electron interactions, and the role of the JT coupling is to change the direction of $\vec{T}_i$, which is much easier.

Now let us turn to the doped case $(x\neq 0)$. The phase boundary J_s(FA) between the spin:F and spin:A increases linearly near $x=0$, has a maximum around $x=0.15$, and turns to decrease with a minimum at around $x=0.30$. The initial increase is due to the difference in the location of the band edges for spin:F and spin:A. This feature remains true even when the spin canting is taken into account because it gives the energy gain only of the order of x^2.[4] Around the maximum of J_s(FA) the curve nature of the spin:A state is changed. For $x<0.15$ the spin structure is stabilized by the super exchange interaction, while it is due to the double exchange one for $x>0.15$ as described above. For $x>0.15$ this phase is orbital:F (x^2-y^2). This is because the orbitals are aligned to maximize the kinetic energy gain, which is realized by the two-dimensional (x^2-y^2) band. Experimentally, in $Nd_{1-x}Sr_xMnO_3$ (Fig. 1), the ferromagnetic metallic phase is realized up to about $x=0.48$ and the charge-exchange (CE)-type AF with the charge ordering turns up around $x=0.5$. With further increasing of x, the metallic state with spin:A appears at about $x=0.53$.[6,7] In this phase the large anisotropy in the electrical resistivity is observed. The similar metallic phase accompanied with spin:A is also found in $Pr_{1-x}Sr_xMnO_3$ $(x>0.48)$ (Refs. 6 and 7) and $La_{1-x}Sr_xMnO_3$ $(x>0.5)$.[13] Since we neglected the long-range Coulomb interaction in the model, the charge ordered phase does not appear in the calculated phase diagram. In the metallic states, however, the screening is effective to make it short ranged and similar to the on-site interactions. Actually the global phase change from the metallic spin:F to the metallic spin:A in Fig. 1 is semiquantitatively in agreement with the calculated phase diagram in Fig. 2 except for the CE-type AF phase with charge ordering. It is worth noting that in spin:A with orbital:F (x^2-y^2) the conduction along the c axis is forbidden in two ways, i.e., by spin and orbital structures. One important consequence is that the spin canting is absent because the kinetic energy gain is forbidden along the c axis even when the spin has the parallel component. This is actually observed experimentally and we regard this as the evidence for the (x^2-y^2)-orbital polarization and the manifestation of the dimensionality control by the orbital degrees of freedom. The fact that the lattice constant along the c axis is smaller compared with those along the a and b axes is also consistent with the (x^2-y^2) orbital in spin:A.[6] We again stress that this phase does not appear when the orbital is not polarized, as in Fig. 2. Furthermore, the effective AF interaction along the c axis is expected to be larger than that in the insulating phase with spin:A $(x=0.0)$, because the ferromagnetic interactions due to the double exchange and super exchange interactions are prohibited along this axis.

As x is further increased in Fig. 2, we have spin:C where the electronic conduction is limited along the c axis. The kinetic energy gain is optimized by the one-dimensional band of orbital:F $(3z^2-r^2)$. Since this one-dimensional band should be very sensitive to disorder, we expect the insulating state as observed experimentally.[6,14] Near the end $x=1$, the spin:G state appears where the energy gain due to the double exchange interaction is absent because the electron motion is blocked in all directions. The electronic energy does not depend on the orbital structures in the limit of strong electron-electron interaction.

We now turn to the ferromagnetic state in Fig. 2. The minimum of J_s(FA) around $x\cong 0.3$ separates rather clearly the two regions dominated by the super exchange $(x\lesssim 0.3)$ and the double exchange interactions $(x\gtrsim 0.3)$. It is worth noting that the origin of the ferromagnetic phase is far from the conventional double exchange mechanism, i.e., both the super exchange interaction and the double exchange one, considerably modified by the orbitals degrees, are relevant in the region $0.2<x<0.4$. As shown in Fig. 2, the orbital structure in spin:F is quite sensitive to the carrier concentration, that is, it changes continuously as x increases from orbital:G $(x^2-y^2)/(3z^2-r^2)$ near $x=0$ to orbital:C $(x^2-y^2)/(3z^2-r^2)$ for $x\cong 0.3$, orbital:A $[(3z^2-r^2)+(x^2-y^2)]/[(3z^2-r^2)-(x^2-y^2)]$ for $0.4<x<0.7$, orbital:F $(3z^2-r^2)$ for $x=0.8$, and finally orbital:F $[(3z^2-r^2)+(x^2-y^2)]$ for $x=0.9$. As a measure we calculated the energy differences among various orbital structures assuming orbital:F, and found it is of the order of $0.01t_0$ per Mn. This is about an order smaller than that in the other spin structures. It suggests the large orbital fluctuations in the ferromagnetic state. This issue has been addressed in Ref. 10 where the character of the orbital fluctuation was studied in the limit of

strong correlation. The two-dimensional flat dispersion for the boson, which represents the orbital degrees, has been found along the three axes in the Brillouin zone. These correspond to the three possible orbital alignments (x^2-y^2), (y^2-z^2), and (z^2-x^2), which suggests the large orbital fluctuation due to the two-dimensional dispersion for boson. Actually there has been no experimental evidence for the orbital ordering in the spin:F state.

If the orbital degrees of freedom are fluctuating and remain disordered, they will play a similar role to that of the spins in the spin liquid near Mott insulators.[15] From this analogy we expect the incoherent charge dymanics in the ferromagnetic metallic state, which has been suggested by various experiments.[1] The orbital entropy should be quenched by the quantum fluctuation, because the specific heat observed experimentally does not show any appreciable residual entropy at low temperature.[16] It suggests the formation of the orbital singlet state without the orbital long-range ordering, which has been discussed in Ref. 17 taking into acount both the the JT coupling[18] and the Coulomb interaction.

In summary, we have studied the role of orbital degeneracy in perovskite manganites $R_{1-x}A_x\mathrm{MnO_3}$ ($R=$La, Pr, Nd, Sm; $A=$Ca, Sr, Ba). The global phase diagram obtained by the mean-field approximation is consistent with the experiments. The essential feature here is the interplay between the super exchange and the double exchange interactions controlled by the orbital degrees of freedom. The dimensionality of the energy band attributed to the orbital structure is important to determine the phase diagram. The large orbital fluctuation is predicted for the ferromagnetic state, where the orbital degrees of freedom play a similar role to that of spin in the doped Mott insulator giving rise to the incoherent charge dymanics.

We thank Y. Tokura, H. Kuwahara, H. Moritomo, S. Maekawa, K. Terakura, and I. Solovyev for their valuable discussions. This work was supported by the Center of Excellence Project from the Ministry of Education, Science and Culture of Japan, and the New Energy and Industrial Technology Development Organization (NEDO).

---

*Present address: Institute for Materials Research, Tohoku University, Sendai, 980-77, Japan.

[1] R. M. Kusters *et al.*, Physica B **155**, 362 (1989); K. Chahara *et al.*, Appl. Phys. Lett. **63**, 1990 (1993); R. von Helmolt *et al.*, Phys. Rev. Lett. **71**, 2331 (1993); S. Jim *et al.*, Science **264**, 413 (1994); Y. Tokura *et al.*, J. Phys. Soc. Jpn. **63**, 3931 (1994); H. Y. Hwang *et al.*, Phys. Rev. Lett. **75**, 914 (1995).

[2] C. Zener, Phys. Rev. **82**, 403 (1951).

[3] P. W. Anderson and H. Hasegawa, Phys. Rev. **100**, 675 (1955).

[4] P.-G. de Gennes, Phys. Rev. **118**, 141 (1960).

[5] N. Furukawa, J. Phys. Soc. Jpn. **63**, 3214 (1994).

[6] H. Kuwahara, Y. Tomioka, and Y. Tokura (private communication).

[7] H. Kawano *et al.*, Phys. Rev. Lett. **78**, 4253 (1997).

[8] H. Kawano *et al.*, Phys. Rev. B **53**, R14 709 (1996).

[9] S. Ishihara, J. Inoue, and S. Maekawa, Phys. Rev. B **55**, 8280 (1997).

[10] S. Ishihara, M. Yamanaka, and N. Nagaosa, Phys. Rev. B **56**, 686 (1997).

[11] J. B. Goodenough, Phys. Rev. **100**, 564 (1955).

[12] K. I. Kugel and D. I. Khomskii, JETP Lett. **15**, 446 (1972).

[13] H. Moritomo *et al.*, Phys. Rev. B **55**, 7549 (1997); T. Akimoto *et al.*, Phys. Rev. B **57**, R5594 (1998).

[14] W. Bao, *et al.*, Phys. Rev. Lett. **78**, 543 (1997).

[15] P. W. Anderson, Science **235**, 1196 (1987).

[16] B. F. Woodfield, M. L. Wilson, and J. M. Byers, Phys. Rev. Lett. **78**, 3201 (1997); T. Okuda and Y. Tokura (private communications).

[17] N. Nagaosa, S. Murakami, and H. C. Lee, Phys. Rev. B **57**, 6767 (1998).

[18] A. J. Millis, P. B. Littlewood, and B. I. Shraiman, Phys. Rev. Lett. **74**, 5144 (1995).